ELSEVIER

International Journal of Solids and Structures 41 (2004) 4423–4434

INTERNATIONAL JOURNAL OF SOLIDS and STRUCTURES

www.elsevier.com/locate/ijsolstr

# Calculations of giant magnetoelectric effect in multiferroic composites of rare-earth-iron alloys and PZT by finite element method

Gang Liu, Ce-Wen Nan *, Ning Cai, Yuanhua Lin

*Department of Materials Science and Engineering, State Key Laboratory of New Ceramics and Fine Processing, Tsinghua University, Tsinghua park, Beijing 100084, China*

Received 26 October 2003; received in revised form 24 March 2004
Available online 27 April 2004

**Abstract**

Magnetoelectric effect of laminated composites of rare-earth-iron alloys (Terfenol-D) and lead–zirconate–titanate (PZT) is calculated by using finite element method. The dependences of the magnetoelectric response on the geometric configuration, the orientations of magnetostriction and polarization, and the applied magnetic field are presented for various sandwiched composites in details. The giant magnetoelectric effect predicted for the Terfenol-D/PZT composites is in agreement with predictions by a recent analytical method and recent experimental observations available.


*Keywords:* Cermets; Magnetoelectricity; Magnetostriction; Piezoelectricity; Finite element analysis

## 1. Introduction

Multiferroic composite materials (Nan and Clarke, 1997; Nan et al., 2002) made by combining ferroelectric and ferromagnetic substances together have drawn significant interest due to their multifunctionality, in which the coupling interaction between ferroelectric and ferromagnetic substances could produce new effects. Recently, the multiferroic composites in the systems of $CoFe_2O_4/BaTiO_3$ (Harshe et al., 1993) and ferrite/lead–zirconate–titanate (PZT) (Bichurin et al., 1997; Srinivasan et al., 2002) have been found to exhibit extrinsic magnetoelectric (ME) effect which is characterized by the appearance of an electric polarization ($ME_H$ output) on applying a magnetic field (Nan, 1994). This extrinsic ME response in the multiferroic composites results from a non-intuitive composite effect, i.e., a $0 + 0 > 0$ composite effect (Nan and Lin, 2002).

The ME effect has been widely investigated in over ten different crystal families (e.g., antiferromagnetic $Cr_2O_3$, yttrium iron garnets, boracites, rare-earth ferrites, and phosphates) (Proceedings of the 3rd

* Corresponding author. Tel.: +86-10-62773300; fax: +86-10-62773587.
*E-mail address:* cwnan@tsinghua.edu.cn (C.-W. Nan).

0020-7683/$ - see front matter © 2004 Elsevier Ltd. All rights reserved.
doi:10.1016/j.ijsolstr.2004.03.022

International Conference on Magnetoelectric Interaction Phenomena in Crystals MEIPIC-3 [Ferroelectrics 1997; 204:1].). However, these monophase ME materials do not exhibit strong ME effect, and most of them have rather low Neel or Curie temperature far below room temperature. These make such single materials difficult to find any practical applications in technology. Alternatively, strong ME effect can be produced in the multiferroic composites as mentioned above. In particular, the ME properties of the composites containing a giant magnetostrictive rare-earth-iron alloy (e.g., $SmFe_2$, $TbFe_2$, or $Tb_{1-x}Dy_xFe_2$ (Terfenol-D) (Engdahl, 2000), which is most widely used magnetostrictive alloy) have recently been calculated (Nan et al., 2001) by developing the Green's function technique (Nan and Clarke, 1997; Nan, 1998; Nan and Weng, 1999), and the predictions have revealed that both particulate composites with Terfenol-D embedded in a piezoelectric matrix such as poly (vinylidene fluoride-trifluorethylene) copolymer [P(VDF-TrFE)] or PZT and laminated composites of Terfenol-D/P(VDF-TrFE) or Terfenol-D/PZT can exhibit a giant ME (GME) effect which is about $10–10^3$ times larger than that in the best known ME materials (such as $Cr_2O_3$ and ferrite/piezoelectric ceramic composites). Subsequently, the laminated Terfenol-D/PZT composite made by stacking and bonding together the PZT and Terfenol-D disks with silver epoxy (Ryu et al., 2001a,b, 2002) and laminated Terfenol-D/PVDF composite made by gluing the polarized PVDF film on Terfenol-D disks with conductive epoxy (Mori and Wuttig, 2002) have been most recently found to exhibit such a GME sensitivity as predicted (Nan et al., 2001), which potentially makes such multiferroic composites particularly attractive for technological applications in actuators, transducers, and sensors.

The GME response of such laminated composites is markedly dependent on the geometric configuration of the laminated composites and the orientations of magnetostriction and polarization in composites. Therefore, for the reason of providing a general guideline for achieving a more progressively desired level of the GME performance, it is urgent to reveal the dependences of the GME response on these important issues explicitly in a quantitative manner. Besides the Green's function technique (Nan et al., 2001), an equivalent circuit approach (Dong et al., 2003a,b) has been recently proposed to simulate the thickness-dependence of the ME response of such sandwiched composites. However, a comprehensive and more accurate understanding on such GME response of the laminated composites is still in lack and the stress/strain transfer from the magnetostrictive phase to the piezoelectric phase is not well shown. In this paper, we employ the finite element method (FEM) and base on the stress/strain transfer to calculate the GME effect in the laminated composite of Terfenol-D and PZT and to present these quantitative dependences of the GME response on the geometric configuration and orientations of magnetostriction and polarization for these laminated composites. Our results are also applicable to other systems such as the laminated composites of PVDF and PZT.

## 2. Theoretical framework

Consider a perfectly bonded Terfenol-D/PZT laminated composite as shown in Fig. 1. The response of the composite involving magnetoelectroelastic coupling effect can be described by the following general equations (Nan et al., 2001):

$$\begin{aligned} \sigma &= \mathbf{c}\varepsilon - \mathbf{e}^{\mathrm{T}}\mathbf{E} - \mathbf{c}\varepsilon^{\lambda}, \\ \mathbf{D} &= \mathbf{e}\varepsilon + \kappa\mathbf{E} + \alpha\mathbf{H}, \\ \mathbf{B} &= \mu(\varepsilon, \mathbf{E}, \mathbf{H})\mathbf{H}, \end{aligned} \tag{1}$$

where $\sigma$, $\varepsilon$, $\mathbf{D}$, $\mathbf{E}$, $\mathbf{B}$ and $\mathbf{H}$ are the stress, strain, electric displacement, electric field, magnetic induction, and magnetic field tensors, respectively; $\mathbf{c}$, $\kappa$ and $\mu$ are, respectively, the elastic stiffness at constant field, dielectric constant tensor at constant strain and permeability tensor at constant strain; the permeability $\mu$ depends on $\varepsilon$, electric and magnetic fields; $\mathbf{e}$ is the piezoelectric coefficient tensor ($\mathbf{e}^{\mathrm{T}}$ being the transpose

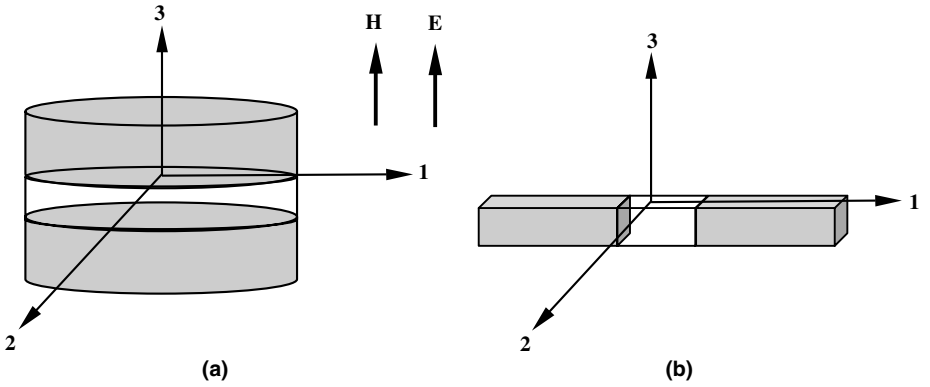


Fig. 1. Triplanar sketch and definition of the coordination axes for (a) disk-shaped composite and (b) block-shaped composite of Terfenol-D and PZT.

of **e**); $\alpha$ is the ME coefficient; $\varepsilon^{\lambda}$ is the magnetostrictively induced strain of Terfenol-D, which is related to the magnetic field dependent magnetostriction constants (Nan and Weng, 1999), $\lambda_{100}$ and $\lambda_{111}$, defined respectively as the change in the normal strain in the [1 0 0] and [1 1 1] crystallographic directions when magnetization is along the [1 0 0] and [1 1 1] directions (Engdahl, 2000).

The strain $\varepsilon$, electric field, and magnetic field are respectively defined by the displacement $u$, electric potential $\varphi$, and magnetic potential $\phi$, i.e.,

$$\varepsilon_{ij} = \tfrac{1}{2}(\boldsymbol{u}_{i,j} + \boldsymbol{u}_{j,i}), \quad \boldsymbol{E}_i = -\varphi_{,i}, \quad \boldsymbol{H}_i = -\phi_{,i}. \tag{2}$$

A state of static equilibrium in the absence of body forces and free electric charges leads to

$$\sigma_{ij,j} = \boldsymbol{0}, \quad \boldsymbol{D}_{i,i} = \boldsymbol{0}, \quad \boldsymbol{B}_{i,i} = 0, \tag{3}$$

where the commas in the subscripts denote partial differentiation with respect to $x_j$, e.g., $\sigma_{ij,j} = \partial\sigma_{ij}/\partial\sigma_j$. In addition, by adopting a similar treatment to what have been successfully applied in the thermoelastoelectric coupling (Tzou and Ye, 1994), the solution procedures for Eq. (1) in the present finite element method are divided into two steps as: (1) calculation of the magnetic field first, and then (2) analysis of the piezoelectricity which is incorporated with the influence from magnetostriction. This treatment is based on the assumption that the magnetic flux density in the composite is dominantly induced by the externally applied magnetic field. After these reasonable simplifications, the finite element formulation can be described as

$$\begin{bmatrix} [\boldsymbol{K}_{uu}] & [\boldsymbol{K}_{u\varphi}] \\ [\boldsymbol{K}_{\varphi u}] & [\boldsymbol{K}_{\varphi\varphi}] \end{bmatrix} \begin{Bmatrix} \{\boldsymbol{u}\} \\ \{\varphi\} \end{Bmatrix} = \begin{Bmatrix} \boldsymbol{F}_u - [\boldsymbol{K}_{uu}]\{\varepsilon^{\lambda}\} \\ \boldsymbol{Q} - [\boldsymbol{K}_{\varphi\phi}]\{\phi\} \end{Bmatrix} \tag{4}$$

where the submatrices $\boldsymbol{K}_{uu}$, $\boldsymbol{K}_{u\varphi}$, $\boldsymbol{K}_{\varphi\varphi}$ and $\boldsymbol{K}_{\varphi\phi}$ indicate the elastic, piezoelectric, permittivity and magnetoelectric coefficient matrices, respectively; $\boldsymbol{F}_u$ and $\boldsymbol{Q}$ represent mechanical excitation vector and electric charge vector, respectively. The left-hand side includes the unknown displacement and electric potential at the vectors; the right-hand includes the excitation of the structure in terms of mechanical loads, applied magnetic loads and electric charge. Based on the above formulation, an eight-node brick finite element was developed and reduced integration was applied selectively for improving the accuracy of the numerical predictions.

The body $\Omega$ could be subjected to either essential or natural mechanical and electric boundary conditions, or combination of them, on its boundary. Here, open circuit and ends clamped in the polarization direction (e.g., the 3-direction in Fig. 1), i.e., $D_3 = 0$ and $\varepsilon_{33} = 0$, are considered to comply with the

experimental conditions. A commercial ANSYS software package was employed to execute the calculations.

## 3. Results and discussion

On applying an external magnetic field $H_3$ alone along the symmetric $\boldsymbol{X}_3$ axis of the composite specimen (Fig. 1), a ME output voltage $E_3$ is produced across the specimen along the $\boldsymbol{X}_3$ direction. Thus the ME sensitivity along the $\boldsymbol{X}_3$ direction, $\alpha_{E33}$, is

$$\alpha_{E33} = -E_3/H_3 = -\alpha^*_{33}/\kappa^*_{33} \tag{5}$$

where $\alpha^*_{33}$ and $\kappa^*_{33}$ are the effective magnetoelectric coefficient and dielectric constant of composites, respectively, and the ME sensitivity $\alpha_{E33}$ represents the figure of merit to assess the performance of a ME material for a magnetic device. The engineering magnetostriction of a Terfenol-D polycrystalline disk, $\varepsilon^{\lambda}$, should be practically determined for a special sample and may be variable from each other (Engdahl, 2000). Here we employ the same $\varepsilon^{\lambda} - \boldsymbol{H}$ behavior as presented before (Nan et al., 2001) and a detailed discussion about the influence of $\varepsilon^{\lambda} - \boldsymbol{H}$ behavior on the ME response will be presented subsequently. $\lambda_{100} = -100$ ppm and $\lambda_{111} = 1700$ ppm at saturation at $\boldsymbol{H}_3 = 2500$ Oe is used for Terfenol-D (Nan et al., 2001; Nan and Weng, 1999). For the polycrystalline Terfenol-D disk, the saturation magnetostrictions parallel and perpendicular $\boldsymbol{H}_3$, $\varepsilon^{\lambda}_{33}$ and $\varepsilon^{\lambda}_{11}$, have been obtained as $\varepsilon^{\lambda}_{11} = \varepsilon^{\lambda}_{22} = -530$ ppm and $\varepsilon^{\lambda}_{33} = 1060$ ppm from the values of $\lambda_{100}$ and $\lambda_{111}$ (Nan and Weng, 1999). Now for quantitative purposes, numerical calculations are carried out for the Terfenol-D/PZT composite. The properties of Terfenol-D and PZT used for calculations are given in Table 1 (Nan et al., 2001).

### 3.1. Effect of geometric configuration of the composites

We first consider three different geometric configurations for the composite as schematically shown in Fig. 2, i.e., disk-shaped sample of one PZT layer sandwiched between two Terfenol-D layers (T–P–T (D), Fig. 2a), disk-shaped sample with one Terfenol-D layer sandwiched between two PZT layers (P–T–P (D), Fig. 2b), and block-shaped sample with one PZT brick bonded between two Terfenol-D bricks (T–P–T (B), Fig. 2c). For calculations, the sizes of the disk-shaped samples are chosen as 12 mm in diameter and 3 mm in thickness as used in experiment (Ryu et al., 2001a,b), and the sizes of the block-shaped samples are $12\times3\times3$ mm. The magnetostrictively induced strain in the Terfenol-D layers is passed along to the PZT

Table 1
Properties of Terfenol-D and PZT-5A used in the present FEM simulations

| Properties | Terfenol-D[a] | PZT-5A[a] |
|---|---|---|
| $\boldsymbol{c}_{11}$ (GPa) | 82 | 121 |
| $\boldsymbol{c}_{12}$ (GPa) | 40 | 75.4 |
| $\boldsymbol{c}_{13}$ (Gpa) | 40 | 75.2 |
| $\boldsymbol{c}_{33}$ (GPa) | 82 | 111 |
| $\boldsymbol{c}_{44}$ (GPa) | 38 | 21.1 |
| $\varepsilon_{11}/\varepsilon_0$ | 6 | 916 |
| $\varepsilon_{33}/\varepsilon_0$ | 6 | 830 |
| $\mu_{33}/\mu_0$ | 5 | 1 |
| $\boldsymbol{e}_{31}$ (C/m$^2$) | 0 | −5.4 |
| $\boldsymbol{e}_{33}$ (C/m$^2$) | 0 | 15.8 |
| $\boldsymbol{e}_{15}$ (C/m$^2$) | 0 | 12.3 |

[a] Nan et al. (2001).

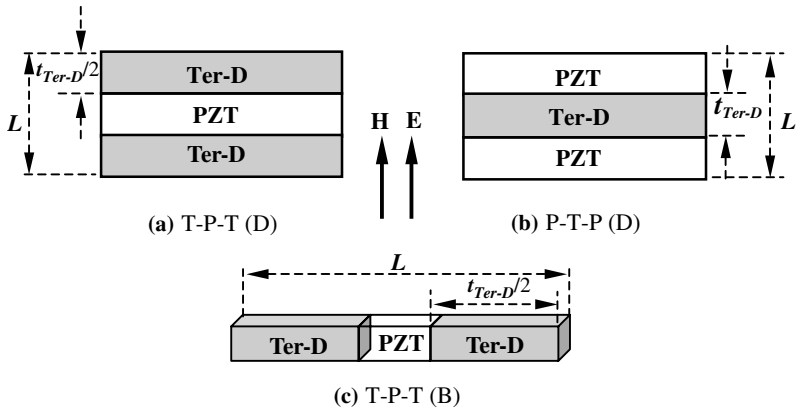


Fig. 2. Schematic illustrations for (a) disk-shaped Terfenol-D/PZT/Terfenol-D composite (T–P–T (D)), (b) disk-shaped PZT/Terfenol-D/PZT composite (P–T–P (D)), and (c) block-shaped Terfenol-D/PZT/Terfenol-D composite (T–P–T (B)). All the Terfenol-D layers have a principal magnetostriction along the 3-direction.

layers, thus resulting in an electric polarization. Fig. 3 shows the dependence of $\alpha_{E33}$ on the thickness or length ratio of Terfenol-D layer to the whole sample, $\boldsymbol{t_{Ter\text{-}D}/L}$ (see Fig. 2).

As seen from Fig. 3, the ME effect of the P–T–P (D) and T–P–T (B) composites are non-monotonically dependent on the $\boldsymbol{t_{Ter\text{-}D}/L}$ with a maximum at $\boldsymbol{t_{Ter\text{-}D}/L} \cong 0.85$, while the ME effect of the T–P–T (D) composite nearly linearly increases with $\boldsymbol{t_{Ter\text{-}D}/L}$. Of particularly interesting to note is that a surprisingly large ME effect, i.e., a GME effect, is produced in all these three laminated composites with thick Terfenol-D layers but thin PZT layers. This trend is in an excellent agreement with that recently predicted by analytical Green's function technique (Nan et al., 2001), and such a GME effect has recently been experimentally observed in the disc-shaped Terfenol-D/PZT/Terfenol-D composite (i.e., a maximum $\alpha_{E33} \sim 5.90$ V/cm Oe at $\boldsymbol{t_{Ter\text{-}D}/L} = 0.8$) (Ryu et al., 2001a,b). The calculated dependence of $\alpha_{E33}$ on the thickness ratio of Terfenol-D phase is also validated in experiment (Ryu et al., 2001a,b). A comparison in Fig. 3 shows that the calculated $\alpha_{E33}$ values are higher than those experimental ones available. The discrepancy between the

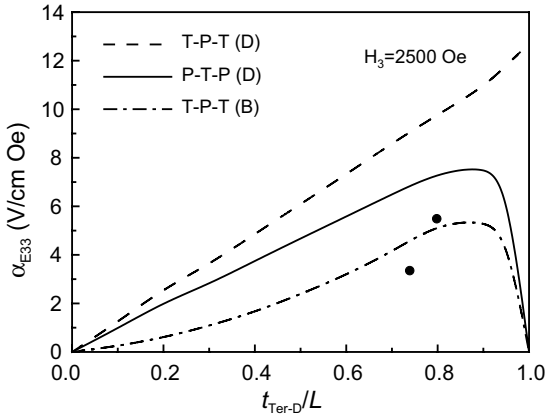


Fig. 3. Dependence of ME sensitivity on thickness or length ratio of Terfenol-D over the whole sample for the sandwiched composites with different configuration as T–P–T (D), P–T–P (D), and T–P–T (B) sketched in Fig. 2. For comparison, two experimental data (solid dots) available for a T–P–T (D) composite (Ryu et al., 2001a,b) are also shown.

calculations and experiment is attributed mainly to the present assumption of a perfect bonding at interface. Any imperfectly interfacial bonding between these Terfenol-D and PZT layers by gluing together would lead to a loss of strain/stress transfers across the interface and thus a drop in $\alpha_{E33}$. Another significant reason for this discrepancy is that the properties (Table 1) of Terfenol-D and PZT, especially the magnetostriction of Terfenol-D, adopted for the present simulation could be different from those in experiment, which are not exactly known.

Compared among the three differently constructed composites, it can be seen from Fig. 3 that the T–P–T (D) sample possesses the most super ME sensitivity while the T–P–T (B) sample the least. In the T–P–T (D) sample, the two outer Terfenol-D layers are also served as metal electrodes, and the effective dielectric constant $\kappa_{33}^{*}$ of the T–P–T (D) sample is equal to $\kappa_{33}^{\mathrm{PZT}}$ of the PZT. For the P–T–P (D) sample, the effective dielectric constant can be simply expressed as

$$\kappa_{33}^{*} = \kappa_{33}^{\mathrm{PZT}}/(1 - \boldsymbol{t}_{\mathbf{Ter\text{-}D}}/\boldsymbol{L}), \tag{6}$$

which is larger than the dielectric constant of the PZT, $\kappa_{33}^{\mathrm{PZT}}$. Thus the T–P–T (D) sample would exhibit a larger $\alpha_{E33}$ than the P–T–P (D) sample with the same $\boldsymbol{t}_{\mathbf{Ter\text{-}D}}/\boldsymbol{L}$. As for the comparison between the sample T–P–T (B) with parallel mode and the series mode sample such as T–P–T (D), a corresponding comparison between calculated effective compressive stress $\sigma_{33}$ in the 3-direction of the two composites, as shown in Fig. 4, illustrates that $\sigma_{33}$ of the T–P–T (B) sample is less than that of T–P–T (D) sample, thereby leading to a lower $\alpha_{E33}$ of the T–P–T (B) than the T–P–T (D) sample.

Under the present boundary conditions, both the absolute sizes, including thickness and diameter or length of all the three samples are found to exert no influences on $\alpha_{E33}$. This hints that, among all the geometric factors of the layered composites, only the relative thicknesses or lengths of Terfenol-D and PZT layers are critical to the ME sensitivity of the composites with perfectly interfacial bonding.

### 3.2. Effect of orientations of magnetization and polarization

There are two orientation cases of the magnetostriction and polarization in the composites. The first one is that the principal magnetostriction of Terfenol-D could be along either the thickness direction or the radial (length) direction so that the laminated composites can be classified into three types (Ryu et al., 2001a,b) as: (a) both Terfenol-D layers having principal magnetostriction along the thickness direction

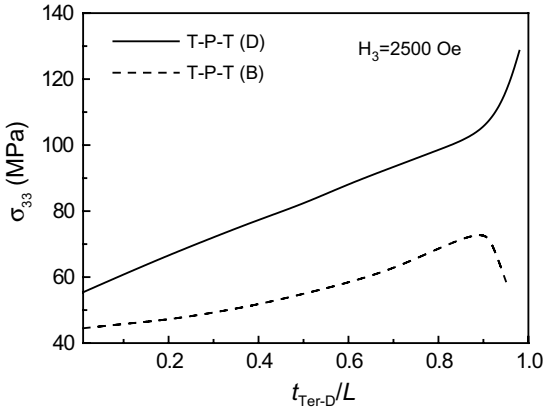


Fig. 4. Variation of predicted effective compressive stress in the 3-direction with the thickness or length ratio of Terfenol-D over the whole sample for the laminated composites of T–P–T (D) and T–P–T (B).

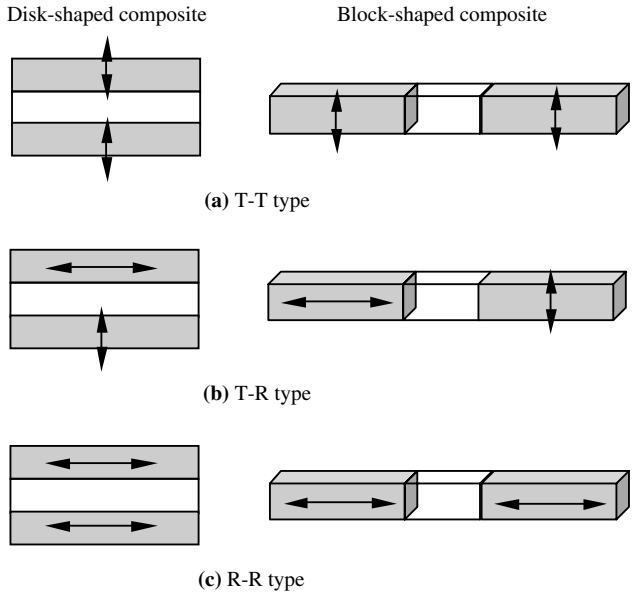


Fig. 5. Sketches of three types of composites with different combination of Terfenol-D having a principal magnetostriction along either thickness direction or radial/length direction, i.e., (a) T–T type, (b) T–R type, and (c) R–R type. The arrows indicate the directions of the principal magnetostriction of Terfenol-D.

(T–T, Fig. 5a), (b) one along the thickness and the other along the radial direction (T–R, Fig. 5b), and (c) both along the radial direction (R–R, Fig. 5c). The polarization direction is still assumed to be along the 3-direction. The second case is shown in Fig. 6, where there is a deflection angle between the directions of applied magnetic field and polarization in the composites. This deflection can be caused either by rotating the dc magnetic field on a stationary sample or by rotating the sample in a stationary dc magnetic field. For calculations, next we rotate the sample but fix the magnetic field direction in present static FEM simulation.

For the first orientation case shown in Fig. 5, the calculations (Fig. 7) explicitly show that the values of $\alpha_{E33}$ for the T–T type composite are comparable with those for the R–R type composite, but both of them

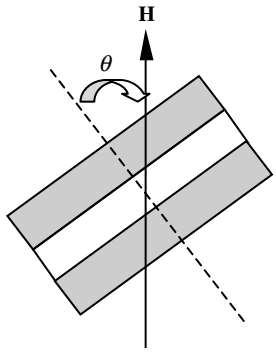


Fig. 6. Schematic illustration of the deflection angle between the directions of externally applied magnetic field and electric polarization.

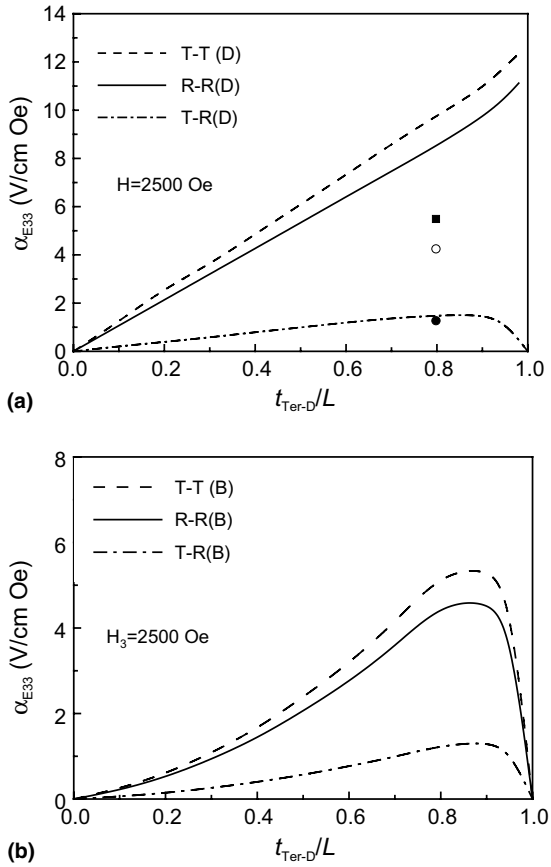


Fig. 7. Comparison of the ME sensitivities of the three types of composites as sketched in Fig. 5 for (a) disk-shaped T–P–T samples and (b) block-shaped T–P–T samples. For comparison, three experimental data (i.e., solid square for R–R type, open dot for T–T type, and solid dot for T–R type composites) available (Srinivasan et al., 2002) are also shown.

exhibit a much larger $\alpha_{E33}$ values than the T–R type composites, which is applicable for both the disk-shaped and the block-shaped composites. The predicted worst ME sensitivity for the T–R type composite has also been observed in experimental (see Fig. 7) (Ryu et al., 2001a,b), but the calculated a little superiority of the T–T type composite over R–R type composite is not in agreement with the available experiment where the R–R type T–P–T (D) composite was found to exhibit a little higher $\alpha_{E33}$ than the T–T type T–P–T (D) composite (Fig. 7). The present boundary condition of mechanically clamped in the 3-direction (polarization direction), which is somewhat different from the free condition in Ryu et al.'s experimental (Ryu et al., 2001a,b), could be the major reason for this little discrepancy. When the ends in the 3-direction are mechanically clamped while the ends in other two directions can move freely the strain or stress in the composite is dominant along the 3-direction due to an intense constraint in this direction. Correspondingly, the output $\boldsymbol{E}_3$ is more dependent on the strain or stress in the clamped 3-direction. The T–T type composites with the principal magnetostriction along the 3-direction are sure to endure more intense stress in the clamped direction than the R–R type composite, as a result, the T–T type composite produces a larger output $\boldsymbol{E}_3$ (see Fig. 8) and thus a larger $\alpha_{E33}$ than the R–R type composites. The reason for the far less ME sensitivity of the T–R type composites is due to a counteracted deformation between the two layers of Terfenol-D. Taking the T–R (D) sample as an example (Fig. 5b), the top layer of Terfenol-D will contract

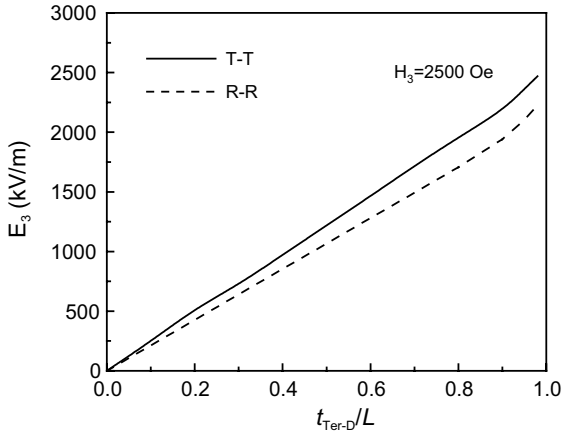


Fig. 8. The variation of the output $E_3$ with the thickness ratio of Terfenol-D over the whole sample for the T–T type and R–R type T–P–T (D) composites, showing that the T–T type one exhibits a larger ME response.

along the clamped direction, then the top interface bonding this Terfenol-D with PZT will move in the 3-direction. The bottom layer of Terfenol-D will expand along the clamped direction, then the bottom interface bonding this Terfenol-D with PZT will move in the 3-direction as well. Such deformations of the two outer Terfenol-D layers will drive the inner PZT layer to move wholly in a troop manner along the 3-direction with a result that the stresses from both top and bottom Terfenol-D are counteracted by each other. This means that no intense stress is imposed on PZT, thus a rather lower ME sensitivity appears in the T–R type composites.

Now let us turn to the second orientation case shown in Fig. 6. The T–T type T–P–T (D) and P–T–P (D) samples with the GME effect are taken as the model composites, and the samples are assumed to rotate in plane and in a counter clockwise way with the magnetic field being stationary, as shown in Fig. 6. Fig. 9 clearly shows that the ME sensitivity of the composites is markedly dependent on the deflection angle $\theta$ between the direction of the externally applied magnetic field and the polarization direction in the composites. The curves of $\alpha_{E33}$ vs $\theta$ seem to be in a form of modified cosine function, and quantitatively, when

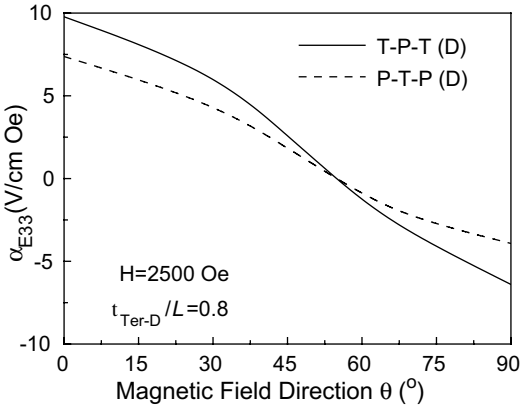


Fig. 9. The dependence of ME sensitivity on the deflection angle between the direction of applied magnetic field and the direction of electric polarization for T–T type T–P–T (D) and P–T–P (D) composites.

the deflection angle increases from 0° to 45°, the $\alpha_{E33}$ values decrease by over three times for both types of samples. It can be concluded that, under the definition of $\theta$, the deflection angle of zero, i.e., the T–T type sample, is the most favorable to produce the GME sensitivity as discussed above (Fig. 7). This is attributed to the reason that, when the principal magnetostriction is parallel with the 3-direction, more constraint should be achieved. Further analyses reveal that the P–T–P (D) samples, although having a little lower ME sensitivity than the T–P–T (D) samples, exhibit a less decrease in $\alpha_{E33}$ with $\theta$. In addition, the calculated relationships of $\alpha_{E33}$ vs $\theta$ are somewhat different from the Ryu et al.'s results (Ryu et al., 2001a,b), which might be due to difference between the present assumption of a mechanically clamped status along the 3-direction and the experimental case of boundary free condition.

### 3.3. Effect of the applied magnetic field

In all the calculations above, we keep the applied magnetic field constant as $\boldsymbol{H}_3 = 2500$ Oe for simplicity. As mentioned above, the engineering Terfenol-D polycrystals may undergo distinct magnetostrictive deformations with the applied magnetic field. For comparison, two different field-dependent magnetostriction constants ($\lambda_{100}$ and $\lambda_{111}$) as presented before (Nan et al., 2001) were used for Terfenol-D (see curves B and C in Fig. 8c of (Nan et al., 2001)). Thus two different field-dependent engineering magnetostrictions, denoted as curves A and B in Fig. 10, have been obtained for the polycrystalline Terfenol-D disks (see curves B and C in Fig. 8b of (Nan et al., 2001)). The T–T type T–P–T and P–T–P samples with $\theta = 0$ are chosen as the model samples.

Fig. 11 shows the calculated dependence of $\alpha_{E33}$ on the magnetic field for the two kinds of Terfenol-D disks (Fig. 10). When the Terfenol-D follows the magnetostriction behavior A where the magnetostriction gets saturation in the low field range, the ME sensitivity of composites will change in a saddle shape with a maximum value in the low magnetic field range (A in Fig. 11). At high magnetic field the magnetostriction becomes saturated, producing a nearly constant electric field, therefore $\alpha_{E33}$ decreases with increasing magnetic field. On the contrary, when the Terfenol-D follows the magnetostriction behavior B where the magnetostriction approaches saturation in high field range, the ME sensitivity of composites monotonically increases (B in Fig. 11). Both trends with bias have been observed in experiments (Ryu et al., 2001a,b; Wan et al., 2003) and are consistent with those predicted by analytical Green's function techniques (Nan et al., 2001). The discrepancy between the two $\alpha_{E33}$ vs $H$ curves (Fig. 11) directly results from the difference between the two magnetostrictive behaviors for Terfenol-D layers (A and B in Fig. 10). Thus the magnetic

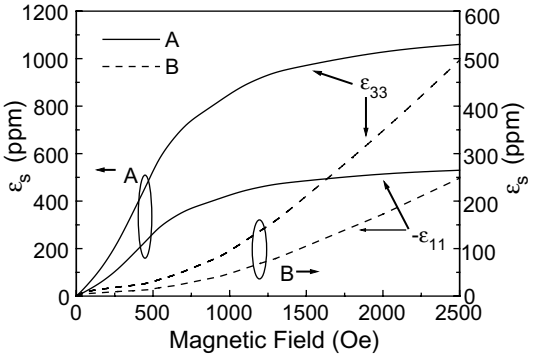


Fig. 10. Two kinds of magnetic field dependences of the magnetostrictive strains adopted for Terfenol-D polycrystals in the present simulation, denoted as A and B, respectively.

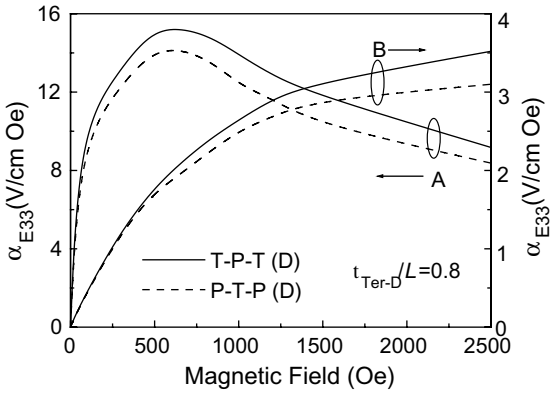


Fig. 11. Dependence of ME sensitivities of the T–T type T–P–T (D) and P–T–P (D) composites on the applied magnetic field. The curves denoted as A and B are corresponding to A and B for Terfenol-D as shown in Fig. 10, respectively.

field dependence of $\alpha_{E33}$ of the composites is dominated by the magnetic field dependence of magnetostriction of the Terfenol-D in the composites.

## 4. Conclusions

The ME effect in the laminated composites of magnetostrictive Terfenol-D stacked and perfectly bonded with piezoelectric PZT has been simulated by finite element method. The calculated GME effect of these sandwiched composites is reasonably agreeable with available experimental results reported recently and recent predictions by the analytical Green's function technique. The results reveal that the ME sensitivity of the laminated composites is strongly dependent on the relative thicknesses or lengths of Terfenol-D and PZT layers. In addition, the externally applied magnetic field is quantitatively found to exert marked influence on the magnetoelectric response not only by intensity variation but also by angle variation. When the applied magnetic field shares the same direction as the polarization, the maximium GME sensitivity is due for the T–T and R–R type laminated composites. When the Terfenol-D behaves in different magnetostriction paths, the variation of magnetoelectric sensitivity with the magnetic field intensity will exhibit as distinct curves. Such a GME sensitivity in the T–T and R–R type laminated composites makes these laminated composites be important materials for magnetic-electric devices, just as the technologically important piezoelectric and magnetostrictive composites extensively investigated.

## Acknowledgements

This work was supported by the State Key Project of Fundamental Research of China (grant no. 2002CB613303 and G2000067108) and from NSFC (grant no. 50232030 and 50172026).

## References

Bichurin, M.I., Kornev, I.A., Petrov, V.M., Lisnevskaya, I., 1997. Investigation of magnetoelectric interaction in composite. Ferroelectrics 204, 289–297.

Dong, S.X., Li, J.F., Viehland, D., 2003a. Giant magneto-electric effect in laminate composites. IEEE Transactions on Ultrasonics Ferroelectrics and Frequency Control, 1236–1239.

Dong, S.X., Li, J.F., Viehland, D., 2003b. Longitudinal and transverse magnetoelectric voltage coefficients of magnetostrictive/piezoelectric laminate composite: theory. IEEE Transactions on Ultrasonics Ferroelectrics and Frequency Control, 1253–1261.

Engdahl, G., 2000. Handbook of Giant Magnetostrictive Materials. Academic Press, New York.

Harshe, G., Dougherty, J.P., Newnham, R.E., 1993. Theoretical modeling of 3-0/0-3 magnetoelectric composites. International Journal of Applied Electromagnetics in Materials 4, 145–171.

Mori, K., Wuttig, M., 2002. Magnetoelectric coupling in Terfenol-D/polyvilylidenedifluoride composites. Applied Physics Letter 81, 100–101.

Nan, C.W., 1994. Magnetoelectric effect in composites of piezoelectric and piezomagnetic phases. Physical Review B 50, 6082–6088.

Nan, C.W., Clarke, D.R., 1997. Effective properties of ferroelectric and/or ferromagnetic composites: a unified approach and its application. Journal of The American Ceramic Society 80, 1333–1340.

Nan, C.W., 1998. Effective magnetostriction of magnetostrictive composites. Applied Physics Letter 72, 2897–2899.

Nan, C.W., Weng, G.J., 1999. Influence of microstructural features on the effective magnetostriction of composite materials. Physical Review B 60, 6723–6730.

Nan, C.W., Li, M., Huang, J.H., 2001. Calculations of giant magnetoelectric effects in ferroic composites of rare-earth-iron alloys and ferroelectric polymers. Physical Review B 63, 144415.

Nan, C.W., Lin, Y., 2002. Microstructure-property linkages in multi-phase ceramics. Key Engineering Materials 224–226, 111–116.

Nan, C.W., Lin, Y.H., Huang, J.H., 2002. Magnetoelectricity of multiferroic composites. Ferroelectrics 280, 319–329.

Ryu, J., Carazo, A.V., Uchino, K., Kim, H.E., 2001a. Magnetoelectric properties in piezoelectric and magnetostrictive laminate composites. Japanese Journal of Applied Physics 40, 4849–4951.

Ryu, J., Priya, S.A., Carazo, A.V., Uchino, K., Kim, H.E., 2001b. Effect of the magnetostrictive layer on magnetoelectric properties in lead zirconate titanate/Terfenol-D composites. Journal of The American Ceramic Society 84, 2905–2908.

Ryu, J., Priya, S.A., Uchino, K., Kim, H.E., 2002. Magnetoelectric effect in composites of magnetostrictive and piezoelectric materials. Journal of Electroceramics, 107–119.

Srinivasan, G., Rasmussen, E.T., Levin, B.J., Hayes, R., 2002. Magnetoelectric effects in ferrite-lead zirconate titanate layered composites: the influence of zinc substitution in ferrites. Physical Review B 65, 134402.

Tzou, H.S., Ye, R., 1994. Piezothermoelasticity and precision control of piezoelectric systems: theory and finite element analysis. Journal of Vibration and Acoustics 116, 489–495.

Wan, J.G., Liu, J.M., Chand, H.L.W., Choy, C.L., Nan, C.W., 2003. Giant magnetoelectric effect of a hybrid of magnetostrictive and piezoelectric composites. Journal of Applied Physics 93, 9916–9919.